ELSEVIER

Applied Mathematical Modelling 24 (2000) 715–732

APPLIED MATHEMATICAL MODELLING

www.elsevier.nl/locate/apm

Dynamics of an elastic ball bouncing on an oscillating plane and the oscillon

James M. Hill *, Michael J. Jennings, Dong Vu To, Kiren A. Williams

School of Mathematics and Applied Statistics, University of Wollongong, Wollongong, NSW 2522, Australia

Received 27 October 1998; accepted 1 December 1999

Abstract

The oscillon is a highly localized dynamical phenomena occurring in a thin horizontal layer of granular material, which rests on a rigid metal plate and the plate oscillates in the vertical direction. It is axially symmetric and physically resembles a splash of liquid due to a falling drop, except that it continually perpetuates itself and does not generate a spreading wave, as is the case for a liquid splash. If the plate vibrates with amplitude A and period $T = 2\pi/\omega$, then the oscillon moves from "peak" to "crater" in time T_1 and "crater" to "peak" time T_2, such that the time from "peak" to "peak" or "crater" to "crater" is twice the period of the oscillating plate namely $T_1 + T_2 = 2T$. At present the physics of granular phenomena is not properly understood and there is no continuum mechanical theory of granular materials which is widely accepted as accurately describing their behavior. Here we present an elementary analysis of a single elastic ball bouncing on an oscillating plate, and we demonstrate that under certain circumstances the ball can perform a "big" bounce followed by a "little" bounce, and then simply repeat the sequence ad infinitum. For a perfectly elastic ball initially at rest on the oscillating plate, the theory with $T_1 = T_2$ predicts oscillonic behavior with an acceleration amplitude $\Gamma = A\omega^2/g$ (g is the acceleration due to gravity) of about 4.6, while experimentally oscillons have been observed to occur for Γ around 2.5. However, for $T_1 \neq T_2$ the theory predicts oscillonic behavior for values of Γ which are well in accord with those observed experimentally. The elementary analysis presented here at least provides specific alternative Γ values for future experimentation, as well providing some insight into what is otherwise a complex physical phenomena.

1. Introduction

Thin layers of sand resting in a vacuum on a rigid horizontal metal plate, are known to form patterns, such as stripes, hexagons, spirals and triangles, when the plate is made to undergo rapid oscillations in a vertical direction. If the metal plate oscillates with amplitude A and angular frequency ω then for certain frequencies $f = \omega/2\pi$ and acceleration amplitudes $\Gamma = A\omega^2/g$ (which are about 30 Hz and 5/2, respectively) so-called "oscillons" appear, which are highly localized structures such that during one cycle a peak occurs and during the next it is a crater and so on (see Fig. 1). If $T = 2\pi/\omega$ is the period of the oscillating plate, then the time from peak to peak or from crater to crater is twice this time. Oscillons were first reported by Umbanhowar et al. [1] and owe their existence to the fact that less energy is dissipated by the grains in a region that is

* Corresponding author. Tel.: +2-4221-3845; fax: +2-4221-4845.
E-mail address: jim_hill@uow.edu.au (J.M. Hill).

0307-904X/00/$ - see front matter
PII: S0307-904X(00)00002-0

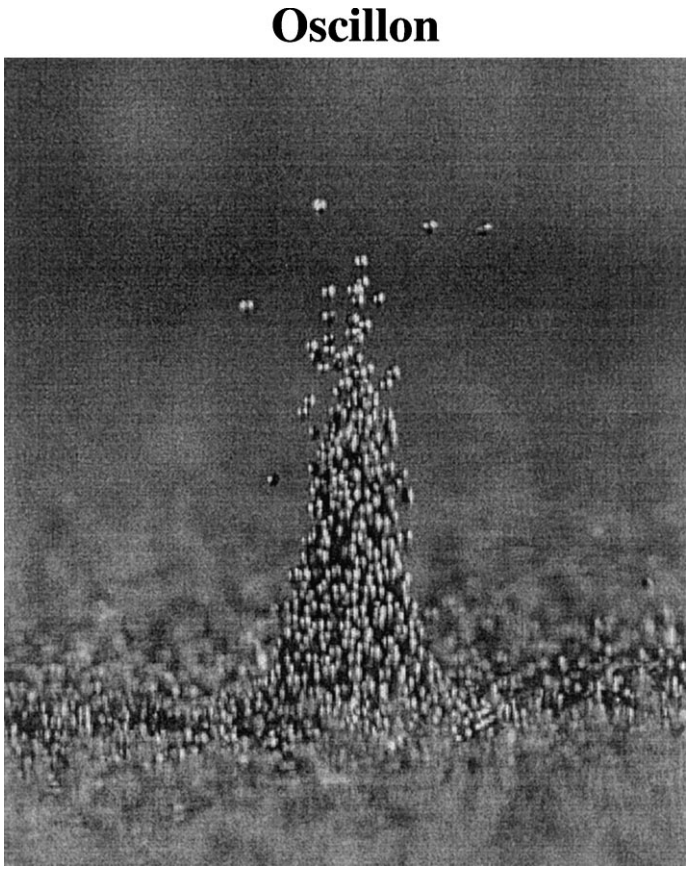

Fig. 1. Oscillon formed from a vibrating layer of brass balls (taking from Paul Umbanhowar's home page http://chaos.ph.utexas.edu/%7Epbu/home.html).

thinner than average, and therefore the grains in a slight depression bounce more vigorously than those around them. Grains in the dip are knocked out to the surrounding region causing a positive feedback which makes a big oscillation in the depression. The closest physical analogy to an oscillon is the "soliton", which is a localized wave of water, arising from the balancing of the linear dispersion term and the nonlinear convective term. In phase oscillons (peaks and craters forming in perfect step) repel each other, while out of phase oscillons attract each other. Attracting oscillons become permanently bound together and more than two oscillons can form stable structures such as chains, triangular associations and extended lattices, and the reader is referred to the general article Chown [2] for further details.

At present modeling granular flow using continuum mechanics is a highly controversial area, on which there is little overall agreement. All granular theories, whether continuum mechanical or otherwise, need to speculate at the microscopic level on the nature of the particle–particle interactions. Since this is presently unknown, the subject is speculative in nature and accordingly somewhat controversial. The problem facing physics and continuum mechanics is to correctly encapsulate behavior at the particle level and yet still produce a tractable and meaningful macroscopic theory. A number of theories have been proposed (see for example [3]) but at this juncture there exists insufficient reliable experimental data to conclude which, if any, of the existing theories are more applicable to real granular systems. Since the physical characteristics of granular materials can vary considerable, the problem of modeling granular flow remains one of

the major outstanding problems of physics and continuum mechanics. Recently, Tsimring and Aranson [4] have proposed a phenomenological model for pattern formation in a vertically vibrated layer of granular material. This is an ad hoc model, not based on continuum mechanics, but the structure and dynamics of solutions closely resemble localized and cellular patterns which are actually observed in experiments.

An elastic ball bouncing on an oscillating plate has been exhaustively studied in the literature, from many points of view, but mainly from the perspective of a simple physical system giving rise to chaotic behaviour. (See for example [5–10] and the numerous references contained therein, especially [5, Chapter 1].) Here, we are not concerned with chaotic behaviour nor with any of the other numerous exotic motions the bouncing ball can follow. Rather, our purpose is to identify conditions under which the motion displays characteristics which closely resemble oscillonic behavior. Under certain circumstances, we show that the ball can make a "big" bounce, followed by a "little" bounce, and then the sequence is repeated, so that we might envisage the big bounce as "peaks" and the little bounce as "craters" and occasionally we use this terminology. There is a simple physical explanation as to why this phenomena should occur. Roughly speaking from the peak the particle has more time to fall and during that time the plate rises significantly but the motion is slowed as it reaches the maximum amplitude and therefore the particle receives less of a "kick". On the other hand, the particle falling from a crater has less time to descend before hitting the plate, but the plate is moving faster and therefore provides the particle with a larger restoring force and it is "kicked" back to the higher position. This explanation is by no means precise, but in order to achieve this repeated pattern of behavior, a synchronization of plate and particle of the type indicated must occur. For a perfectly elastic particle initially at rest on the plate, the simple theory with $T_1 = T_2$, predicts almost oscillonic behavior with an acceleration amplitude Γ which exceeds those which have been observed to occur experimentally. However, for other coefficients of restitution and $T_1 \neq T_2$, the theory predicts values of Γ which are well in accord with experimental observations. Moreover, it also predicts other values of Γ for which almost oscillonic behavior can be expected to occur. In fact for almost oscillonic behavior there are an infinite family of such allowable Γ's such that the necessary acceleration amplitudes might be be termed "quantized". Alternatively, we can produce precise oscillonic behavior simply by locating the particle at one of the stationary positions and allowing it to fall freely under gravity at some designated time t_0.

We employ the elementary theory of particles falling vertically under gravity, and for impacts with the plate we adopt the standard constitutive law

$$|\text{relative velocity after impact}| = e|\text{relative velocity before impact}|, \tag{1}$$

where e denotes the usual coefficient of restitution. In Section 2, for a particle initially at rest on the plate, we examine the initial motion of the particle, which is a separate calculation, and the time t_0 to the first stationary position and the corresponding height z_0 turn out to be particularly important parameters. The suggested motion is only possible if initially the particle is propelled into one of the crater or peak locations. If it is not located initially in one of these two modes, then some other motion eventuates. The constraints on t_0 and z_0 provide two equations, one of which prescribes the acceleration amplitude while the other represents essentially a consistency condition which must be satisfied in order to obtain oscillonic behavior. Since this latter condition is satisfied only approximately, we term the motion "almost" oscillonic. In Section 3, we detail the subsequent motion between peaks and craters and vice versa to determine precise conditions under which a motion of this type is possible. In general, the problem reduces to solving the nonlinear system of three equations (37) for the three unknowns x_0, x_1 and x_2 which are defined by Eq. (36). In Section 4 we show that the special case when $T_1 = T_2 = T$ is only possible for the

perfectly elastic ball ($e = 1$) and some detailed numerical results for this case are presented. In Section 5 we detail the solution of (37) for the case $T_1 \neq T_2$, and numerical results for this general case gives rise to values of Γ which are precisely in accord with the experimental values obtained for the oscillon.

2. Initial motion of the particle

We consider the idealized situation of a ball bouncing vertically on a horizontal rigid metal plate which is performing oscillations in the vertical direction according to $z(t) = A\sin\omega t$ and the vertically upwards direction is taken to be positive. We assume that the particle remains in a vertical plane and that initial motion occurs at time t_c $(0 \leqslant \omega t_c \leqslant \pi/2)$ as a result of the particle leaving the plate from originally being at rest on the stationary plate. For $0 \leqslant t \leqslant t_c$, the particle remains on the plate and has the equation of motion

$$M\frac{d^2z}{dt^2} = N - Mg, \tag{2}$$

where M is the mass of the particle and N is the normal reaction between the particle and the plate, as indicated in Fig. 2. The particle remains on the plate so long as $N > 0$ but leaves the plate when $N = 0$ at time t_c which is determined for the condition

$$A\omega^2\sin\omega t_c = g, \tag{3}$$

or alternatively

$$\omega t_c = \sin^{-1}(1/\Gamma), \tag{4}$$

where $\Gamma = A\omega^2/g$, is assumed to be greater than unity. The position and velocity of the particle are known at t_c and for $t \geqslant t_c$ the subsequent motion of the particle is described by

$$\begin{aligned} z(t) &= \frac{A}{\Gamma} + \frac{A}{\Gamma}\omega\left(\Gamma^2 - 1\right)^{1/2}(t - t_c) - \frac{g}{2}(t - t_c)^2, \\ v(t) &= \frac{A}{\Gamma}\omega\left(\Gamma^2 - 1\right)^{1/2} - g(t - t_c), \end{aligned} \tag{5}$$

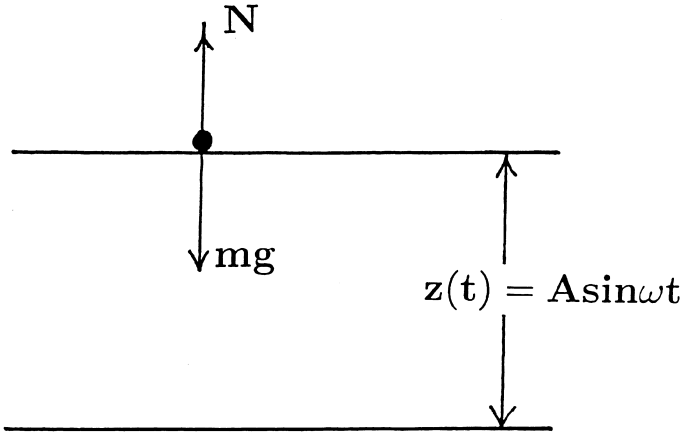

Fig. 2. Particles of mass m initially resting on a horizontal plate which is moving according to $z(t) = A\sin\omega t$.

where $v(t) = \mathrm{d}z/\mathrm{d}t$ denotes the velocity of the particle. From these equations we may deduce that the time t_0 be the first stationary point and the particle height z_0 at that time are given by

$$\omega t_0 = \sin^{-1}(1/\Gamma) + \left(\Gamma^2 - 1\right)^{1/2}, \quad z_0 = A\left(\Gamma^2 + 1\right)/2\Gamma, \tag{6}$$

which are important parameters which we exploit later. In the following section we analyze the motion between peaks and craters and vice versa.

3. Motion between peaks and craters and vice versa

Suppose that t_n and z_n denote the time and position respectively at which the particle has zero velocity. Since for time $t \geqslant t_n$ the particle falls under gravity, its position and velocity are given respectively by

$$z(t) = z_n - \frac{g}{2}(t - t_n)^2, \quad v(t) = -g(t - t_n). \tag{7}$$

Let $\tau_n \geqslant t_n$ be the time at which the particle collides with the plate, so that τ_n is determined as a root of the transcendental equation

$$z_n - \frac{g}{2}(\tau_n - t_n)^2 = A \sin \omega\tau_n. \tag{8}$$

Fig. 3 shows the particle falling downwards with a velocity of magnitude u_1, and rebounding vertically upwards with a velocity of magnitude v. In Fig. 3(a) the plate is assumed moving upwards with velocity u_2 while in Fig. 3(b) it is assumed to be moving downwards but $u_1 > u_2$. Application of the physical law (1) to both situations gives respectively

$$v - u_2 = e(u_1 + u_2), \quad v + u_2 = e(u_1 - u_2),$$

or alternatively

$$v = eu_1 + (1 + e)u_2, \quad v = eu_1 - (1 + e)u_2.$$

Thus, with our sign convention, if v_1 is the particle velocity, v_2 the plate velocity, then both formulae combine to give the rebound particle velocity v as

$$v = -ev_1 + (1 + e)v_2, \tag{9}$$

which we adopt as the basic equation to determine the particle velocity after impact with the plate. From (7) and (9) we have

$$v(\tau_n) = eg(\tau_n - t_n) + (1 + e)A\omega \cos \omega\tau_n, \tag{10}$$

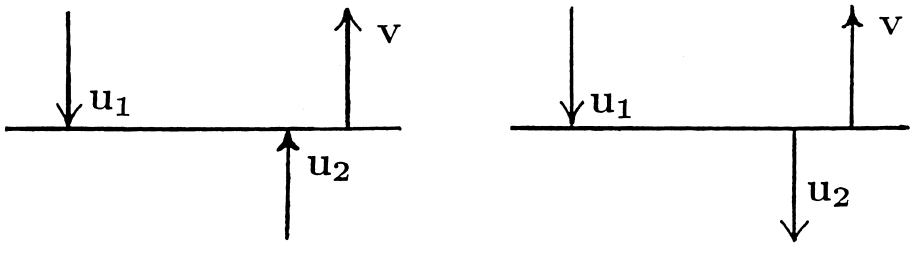

Fig. 3. Falling particles impacting on both upwards and downwards moving plate, arrows indicating direction of movement: (a) plate moving upwards; (b) plate moving downwards and $u_1 > u_2$.

and for $t \geqslant \tau_n$, the position and velocity of the particle are given respectively by

$$z(t) = z(\tau_n) + v(\tau_n)(t-\tau_n) - \frac{g}{2}(t-\tau_n)^2, \quad v(t) = v(\tau_n) - g(t-\tau_n). \tag{11}$$

From these equations it is a simple matter to deduce

$$t_{n+1} = \tau_n + \frac{v(\tau_n)}{g}, \quad z_{n+1} = z(\tau_n) + \frac{v(\tau_n)^2}{2g}, \tag{12}$$

so that we obtain, using (7), the relation

$$\begin{aligned} z_{n+1} &= z_n - \frac{g}{2}(\tau_n - t_n)^2 + \frac{g}{2}(t_{n+1} - \tau_n)^2, \\ &= z_n + \frac{g}{2}(t_{n+1} - t_n)[(t_n + t_{n+1}) - 2\tau_n], \end{aligned}$$

from which we may deduce

$$\tau_n = \frac{(t_n + t_{n+1})}{2} - \frac{(z_{n+1} - z_n)}{g(t_{n+1} - t_n)}, \tag{13}$$

a result which is independent of the assumed physical law given by Eq. (1).

Now t_0 and z_0 denote the time and position to the first stationary point. We now suppose T_1 is the time to the subsequent stationary point occurring at time t_1 and position z_1. Further, we let T_2 be the time to the next stationary point which occurs at time t_2 and position z_2. We now assume that this pattern is repeated for $n \geqslant 0$

$$t_{2n} = n(T_1 + T_2) + t_0, \quad t_{2n+1} = n(T_1 + T_2) + t_0 + T_1, \tag{14}$$

and that if h_1 and h_2 denote the heights at times t_1 and t_2, respectively we have

$$z_{2n} = h_2 (n \geqslant 1), \quad z_{2n+1} = h_1 (n \geqslant 0). \tag{15}$$

From (13)–(15), with $T_1 + T_2 = 2T$ we may deduce

$$\begin{aligned} \tau_{2n} &= 2nT + t_0 + \frac{T_1}{2} - \frac{(h_1 - h_2)}{gT_1}, \\ \tau_{2n+1} &= (2n+1)T + t_0 + \frac{T_1}{2} + \frac{(h_1 - h_2)}{gT_2}, \end{aligned} \tag{16}$$

and using Eqs. (8) and (10) in conjunction with (14)–(16) gives rise to the four basic equations prescribing the motion.

From (8) and (10) and the first equations of (14)–(16) we can deduce

$$\begin{aligned} h_2 - \frac{g}{2}\left\{\frac{T_1}{2} - \frac{(h_1 - h_2)}{gT_1}\right\}^2 &= A\sin\omega\left\{2nT + t_0 + \frac{T_1}{2} - \frac{(h_1 - h_2)}{gT_1}\right\}, \\ \rho g\frac{T_1}{2} + \frac{(h_1 - h_2)}{T_1} &= A\omega\cos\omega\left\{2nT + t_0 + \frac{T_1}{2} - \frac{(h_1 - h_2)}{gT_1}\right\}, \end{aligned} \tag{17}$$

where the constant ρ is defined by

$$\rho = \left(\frac{1-e}{1+e}\right). \tag{18}$$

Now since the left-hand sides of (17) are independent of n, such a motion is only possible if $\omega T = m\pi$, for some integer m. Here, we have in mind the period doubling case $m = 2$, but for the time being we leave m arbitrary. Assuming that $\omega T = m\pi$, (17) becomes

$$\begin{aligned} h_2 - \frac{g}{2}\left\{\frac{T_1}{2} - \frac{(h_1 - h_2)}{gT_1}\right\}^2 &= A\sin\omega\left\{t_0 + \frac{T_1}{2} - \frac{(h_1 - h_2)}{gT_1}\right\}, \\ \rho g\frac{T_1}{2} + \frac{(h_1 - h_2)}{T_1} &= A\omega\cos\omega\left\{t_0 + \frac{T_1}{2} - \frac{(h_1 - h_2)}{gT_1}\right\}, \end{aligned} \tag{19}$$

and in a similar manner, from (8) and (10) and the second equations of (14)–(16) we obtain

$$\begin{aligned} h_1 - \frac{g}{2}\left\{\frac{T_2}{2} + \frac{(h_1 - h_2)}{gT_2}\right\}^2 &= A\sin\omega\left\{t_0 - \frac{T_2}{2} + \frac{(h_1 - h_2)}{gT_2}\right\}, \\ \rho g\frac{T_2}{2} - \frac{(h_1 - h_2)}{T_2} &= A\omega\cos\omega\left\{t_0 - \frac{T_2}{2} + \frac{(h_1 - h_2)}{gT_2}\right\}. \end{aligned} \tag{20}$$

Eqs. (19) and (20), together with the constraint

$$\omega(T_1 + T_2) = 2m\pi, \tag{21}$$

constitute five equations for the five unknown quantities T_1, T_2, h_1, h_2 and t_0 assuming that A, ω, ρ and m are all prescribed.

The form of (19) and (20) suggest we introduce δ_1 and δ_2 such that

$$\delta_1 = \frac{T_1}{2} - \frac{(h_1 - h_2)}{gT_1}, \quad \delta_2 = \frac{T_2}{2} - \frac{(h_1 - h_2)}{gT_2}, \tag{22}$$

and on rearranging somewhat, the four basic equations (19) and (20) can be shown to become

$$\begin{aligned} h_2 &= \frac{g}{2}\delta_1^2 + A\sin\omega(t_0 + \delta_1) = \frac{g}{2}\delta_2^2 + A\sin\omega(t_0 - \delta_2), \\ T_1 &= \frac{2}{(1+\rho)}\left\{\delta_1 + \frac{A\omega}{g}\cos\omega(t_0 + \delta_1)\right\}, \\ T_2 &= \frac{2}{(1-\rho)}\left\{\delta_2 - \frac{A\omega}{g}\cos\omega(t_0 - \delta_2)\right\}. \end{aligned} \tag{23}$$

In addition, from (22) and on equating expressions for $(h_1 - h_2)$ and using (21) we may deduce the equation

$$T_1 - T_2 = \frac{\omega}{m\pi}\{\delta_1 T_1 - \delta_2 T_2\}. \tag{24}$$

Eqs. (21), (23) and (24) comprise five relations for the determination of the five quantities T_1, T_2, δ_1, δ_2 and t_0. In the following section we detail a particularly simple solution of these equations for which $T_1 = T_2$ (and therefore $\delta_1 = \delta_2$) but only applying to the case of a perfectly elastic ball ($e = 1$).

4. Special case of $T_1 = T_2$ for a perfectly elastic ball

Now assuming $T_1 = T_2$, it follows from (22) that $\delta_1 = \delta_2$ and therefore from the first equations of (23) we have either $\cos\omega t_0 = 0$ or $\sin\omega\delta = 0$. The latter case is of no physical interest while in the former case we have $\omega t_0 = (2k+1)\pi/2$ for some integer k and from (23) we obtain

$$T_1 = \frac{2}{(1+\rho)}\left\{\delta - \frac{A\omega}{g}(-1)^k \sin\omega\delta\right\},$$
$$T_2 = \frac{2}{(1-\rho)}\left\{\delta - \frac{A\omega}{g}(-1)^k \sin\omega\delta\right\}, \tag{25}$$

which coincide if and only if ρ is zero in which case we have

$$T_1 = T_2 = 2\left\{\delta - \frac{A\omega}{g}(-1)^k \sin\omega\delta\right\}. \tag{26}$$

On using (21) we can deduce

$$\frac{m\pi}{2} - \delta\omega = (-1)^{k+1}\Gamma \sin\omega\delta, \tag{27}$$

as the determining equation for δ and where $\Gamma = A\omega^2/g$. On introducing the parameter λ defined by

$$\lambda = \frac{(h_1 - h_2)\omega^2}{m\pi g}, \tag{28}$$

we have on using $T_1 = T_2 = m\pi/\omega$ and (22), the following relation

$$\lambda = \left\{\frac{T^2}{2} - \delta T\right\}\frac{\omega^2}{m\pi} = \frac{m\pi}{2} - \delta\omega, \tag{29}$$

and therefore from (27) we obtain

$$\lambda = (-1)^{k+1}\Gamma\left\{\sin\frac{m\pi}{2}\cos\lambda - \cos\frac{m\pi}{2}\sin\lambda\right\}. \tag{30}$$

Thus if $m = 2p$ for some integer p we have

$$\lambda = (-1)^{k+p}\Gamma \sin\lambda, \tag{31}$$

while if $m = 2p + 1$ we obtain

$$\lambda = (-1)^{k+p}\Gamma \cos\lambda. \tag{32}$$

Now in the particular physical situation of interest $m = 2$ ($p = 1$) and assuming that λ is determined as a root of equation (31) with $p = 1$, then h_2 is found from (23), thus

$$\frac{h_2\omega^2}{g} = (-1)^{k+1}\Gamma\cos\lambda + \frac{1}{2}(\pi - \lambda)^2. \tag{33}$$

Now a motion of this type can only occur if Γ and ω are such that t_0 and z_0 as given by Eq. (6) satisfy

$$\sin^{-1}(1/\Gamma) + (\Gamma^2 - 1)^{1/2} = (2k+1)\pi/2, \quad A(\Gamma^2+1)/2\Gamma = \{h_1, h_2\}, \tag{34}$$

and in principle these latter conditions constitute two equations for the determination of the necessary A and ω, which allow oscillonic motion of the type described. However, Eq. $(34)_1$, defines Γ but equation $(34)_2$ turns out to define the quantity $h_2\omega^2/g$, which is already defined by Eq. (33) and a similar situation occurs for the case when z_0 is set to equal h_2.

Fig. 4, which is given by Umbanhowar et al. [1], shows the region of acceleration amplitudes $\Gamma = A\omega^2/g$ and frequencies $f = \omega/2\pi$ where oscillons and other patterns have been observed to occur experimentally. It is clear that oscillons arise for Γ approximately 2.5 and f in the range

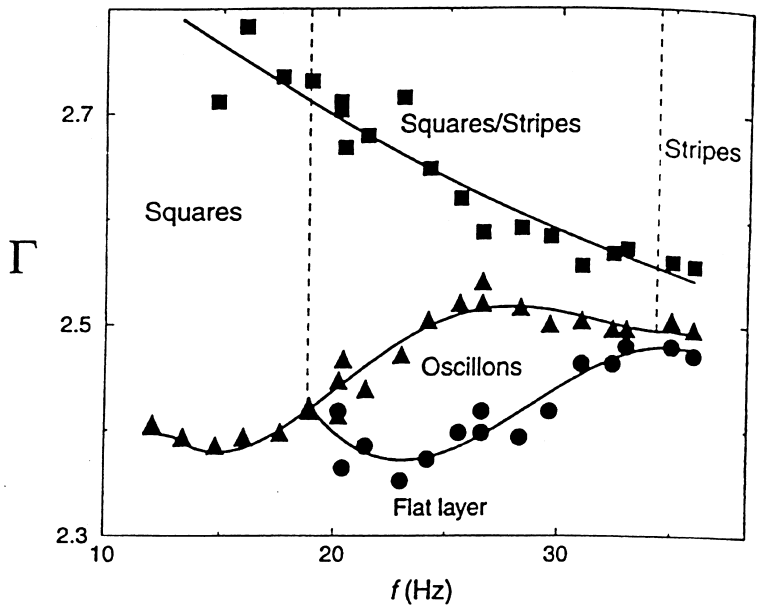

Fig. 4. Diagram showing the stability regions for different states (from [1]).

Table 1
Numerical values of Γ, λ, Δ_1, and Δ_2 for various values of k[a]

k	Γ	λ	Δ_1	Δ_2
1	4.60	2.55*	−1.30*	14.72
2	7.79	3.63*	1.04*	23.84
		5.50*	−0.98*	33.58
3	10.95	2.88	52.90	70.99
		6.97*	0.86*	44.66
		8.53*	−0.81*	52.79
4	14.10	3.38	64.94	86.18
		5.86	72.25	109.07
		10.24*	0.70*	65.04
		11.60*	−0.74*	72.15
5	17.25	2.97	147.60	166.26
		6.68	85.14	127.11
		8.88	91.77	147.57
		13.46*	0.67*	85.24
		14.69*	−0.64*	91.66
6	20.40	3.30	167.69	188.42
		5.99	186.42	224.05
		9.93	105.30	167.69
		11.94	111.38	186.40
		16.66*	0.70*	105.37
		17.79*	−0.50*	111.27

[a] Γ is obtained from $(34)_1$, λ from (31) and Δ_1 and Δ_2 from (35).

20–35 Hz. For integer $k \geqslant 1$, we solve Eq. $(34)_1$ to determine Γ and then λ is obtained by solving Eq. (31) with $p = 1$ and the numerical results are shown in Table 1. Fig. 5 shows the determination of the roots of equation (31) for various values of k, the straight lines having gradients

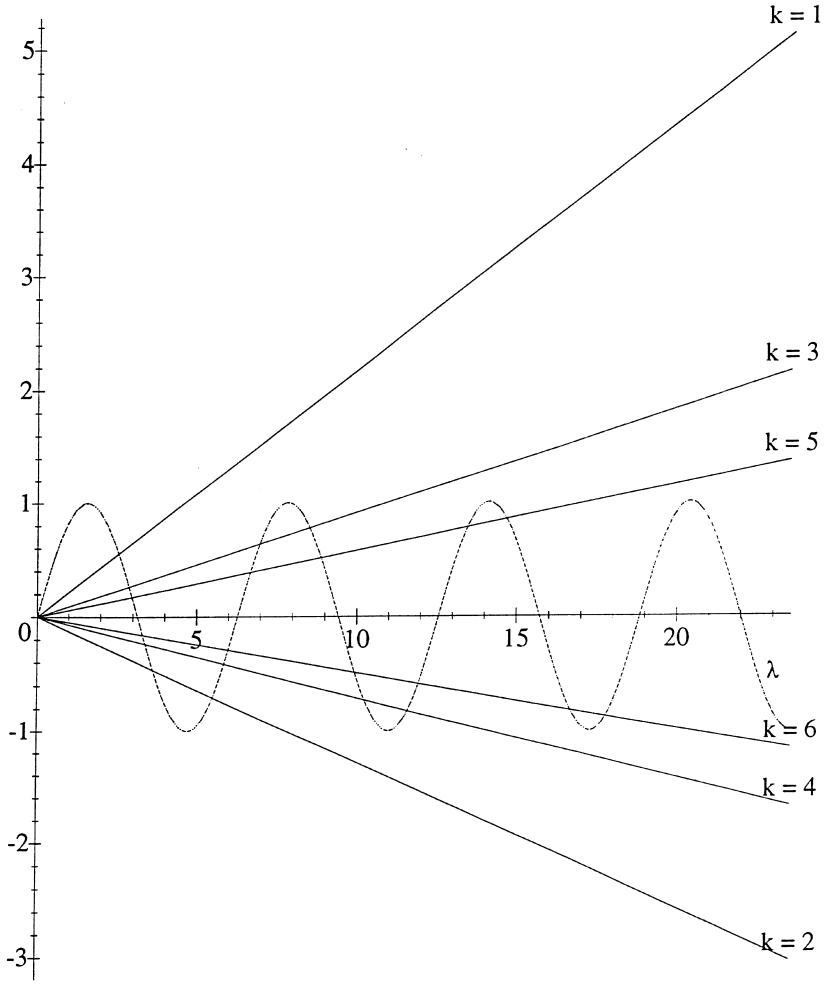

Fig. 5. Determination of the roots of equation (31) (with $p = 1$) as the intersection of $\sin\lambda$ and the straight lines of gradient $(-1)^{(k+1)}/\Gamma$.

$(-1)^{(k+1)}/\Gamma$. For precise oscillonic behavior we require the initial height z_0 to be either of h_1 or h_2 as indicated by Eq. $(34)_2$. However, our theory does not allow this as a "precise" outcome and the final two columns of Table 1 show the numerical values of Δ_1 and Δ_2 which are defined respectively by

$$\begin{aligned}\Delta_1 &= \frac{\omega^2(z_0 - h_1)}{g} = \frac{1}{2}\left\{(\Gamma^2+1) + (-1)^k 2\Gamma\cos\lambda - (\pi+\lambda)^2\right\},\\ \Delta_2 &= \frac{\omega^2(z_0 - h_2)}{g} = \frac{1}{2}\left\{(\Gamma^2+1) + (-1)^k 2\Gamma\cos\lambda - (\pi-\lambda)^2\right\}.\end{aligned} \tag{35}$$

Clearly, from Table 1 it is apparent that z_0 can be almost h_1 but never h_2, and in view of the large values of ω of interest experimentally, it is clear that $z_0 \simeq h_1$ and such values are indicated in Table 1 with an asterisk. In Appendix A we present asymptotic formulae for large values of Γ which confirm the behavior indicated in Table 1.

5. Solution for any T_1, T_2 and coefficient of restitution e

On introducing three non-dimensional variables x_0, x_1 and x_2 defined by

$$x_0 = \omega t_0, \quad x_1 = \omega\delta_1, \quad x_2 = \omega\delta_2, \tag{36}$$

where δ_1 and δ_2 are defined by Eq. (22), then from (23), on eliminating T_1 and T_2 by means of the two relations (21) and (24), we obtain the following three determining equations:

$$\begin{aligned}
&\frac{1}{2}\left(x_1^2 - x_2^2\right) + \Gamma\{\sin(x_1 + x_0) + \sin(x_2 - x_0)\} = 0,\\
&x_1 + \Gamma\cos(x_1 + x_0) = \frac{m\pi(1+\rho)(x_2 - m\pi)}{(x_1 + x_2 - 2m\pi)},\\
&x_2 - \Gamma\cos(x_2 - x_0) = \frac{m\pi(1-\rho)(x_1 - m\pi)}{(x_1 + x_2 - 2m\pi)},
\end{aligned} \tag{37}$$

where as before $\Gamma = A\omega^2/g$ and x_0 and Γ are related by Eq. $(6)_1$. In this terminology the solution of the previous section for ρ zero is simply $x_1 = x_2 = x$, where x satisfies

$$\frac{m\pi}{2} - x = (-1)^{k+1}\Gamma\sin x, \tag{38}$$

which is the same equation as (27). A numerical solution of the system (37) can be obtained directly, but some formal simplification can be achieved giving rise in particular to the important equation (42), which shows that if $e = 1$, then $x_1 = x_2$ unless the denominator on the right-hand side of (42) vanishes. Further, Eq. (42) shows that for m even (say $m = 2p$), $x_1 = x_2 = p\pi$ is a root for all values of the coefficient of restitution.

On introducing new variables

$$x = \frac{1}{2}(x_1 + x_2), \quad y = \frac{1}{2}(x_1 - x_2), \tag{39}$$

so that we have

$$x_1 = x + y, \quad x_2 = x - y, \tag{40}$$

which simplifies the system (37) to yield

$$\begin{aligned}
&xy + \Gamma\sin x\cos(y + x_0) = 0,\\
&x - \Gamma\sin x\sin(y + x_0) = \frac{m\pi}{2}\left\{1 - \frac{\rho y}{(x - m\pi)}\right\},\\
&y + \Gamma\cos x\cos(y + x_0) = \frac{m\pi}{2}\left\{\rho - \frac{y}{(x - m\pi)}\right\},
\end{aligned} \tag{41}$$

and on eliminating $\Gamma\cos(y + x_0)$ from the first and third of these, we can deduce

$$y = \frac{m\pi}{2}\rho\left\{\left(\frac{x - (m\pi/2)}{x - m\pi}\right) - x\cot x\right\}^{-1}, \tag{42}$$

which shows that if ρ is zero then $x_1 = x_2$, but note that this does not necessarily mean that $T_1 = T_2$. This is one possibility, but there is also another as can be deduced from Eq. (22).

A final determining equation for x can be obtained by eliminating x_0 using the standard relation $\sin^2(y + x_0) + \cos^2(y + x_0) = 1$, and it is convenient to introduce new variables

$$X = x - \frac{m\pi}{2}, \quad \alpha = \frac{m\pi}{2}. \tag{43}$$

From $(41)_2$, $(41)_1$ and (42) we can deduce

$$\begin{aligned} \Gamma \sin x \sin(y + x_0) &= X + \frac{(\alpha\rho)^2}{\{X - (X^2 - \alpha^2)\cot x\}}, \\ \Gamma \sin x \cos(y + x_0) &= \frac{\alpha\rho(X^2 - \alpha^2)}{\{X - (X^2 - \alpha^2)\cot x\}}. \end{aligned} \tag{44}$$

We note that these equations formally yield (38) in the limit ρ tending to zero. On squaring and adding we finally obtain a single equation for the determination of X and from which all other quantities may be found, namely

$$\begin{aligned} &\Gamma^2\left\{X\sin(X+\alpha) - \left(X^2 - \alpha^2\right)\cos(X+\alpha)\right\}^2 \\ &\quad = \left\{X^2 - X\left(X^2 - \alpha^2\right)\cot(X+\alpha) + (\alpha\rho)^2\right\}^2 + (\alpha\rho)^2\left(X^2 - \alpha^2\right)^2, \end{aligned} \tag{45}$$

and this equation would need to be solved numerically.

The appearance of the trigonometric functions in (37) means that the system no doubt possess numerous solutions, and we emphasize here that we make no attempt to provide an exhaustive investigation. We merely demonstrate how certain families of solutions relate to the results of the previous section and we establish that this set of equations has solutions for those Γ values which are observed in the oscillon experiments. From using a multi-dimensional Newton–Raphson scheme, Figs. 6 and 7 each show the variation of allowable Γ values with e for three distinct families of solutions of (37), which for $e = 1$ all coincide with the first two Γ values given in Table 1. Numerical values of the roots x_0, x_1 and x_2 corresponding to Figs. 6 and 7 are given in Tables 2 and 3, respectively. Notice that the root $x_1 = x_2 = \pi$ occurs in both tables for all values of the coefficient of restitution and the validity of this root can be verified directly from Eq. (42). Fig. 8 shows the variation of Γ with e for one family of solutions and the corresponding numerical

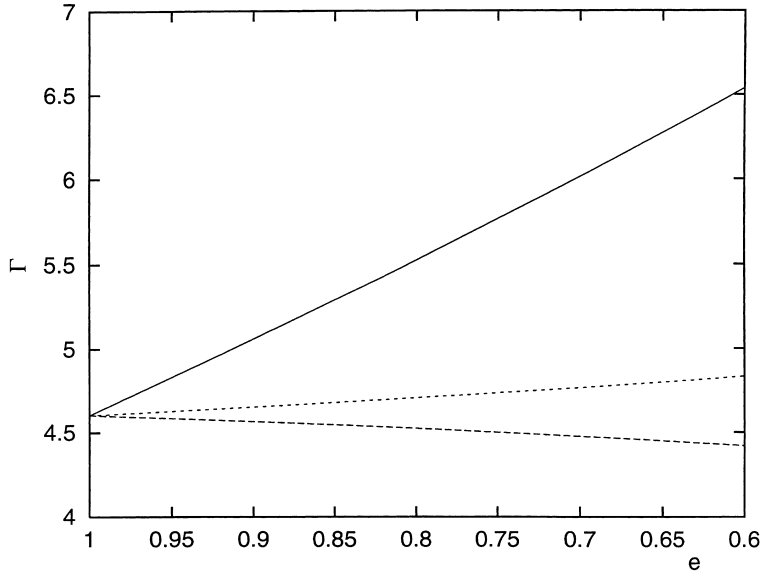

Fig. 6. Variation of Γ with e for three families of solutions of the system (37) which all pass through the value $\Gamma = 4.60$.

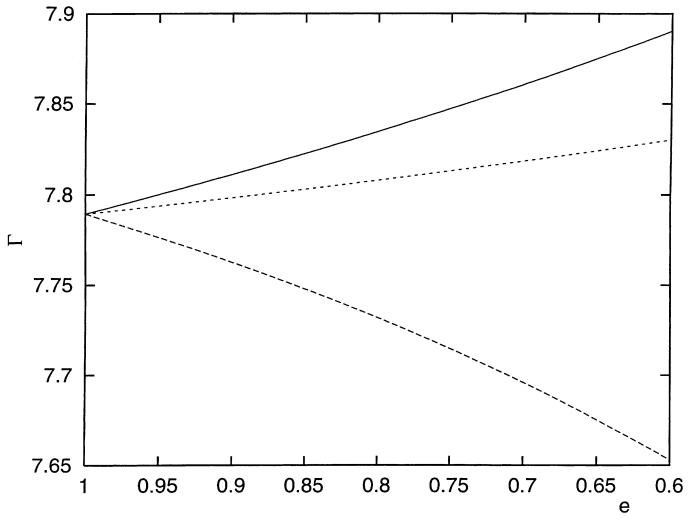

Fig. 7. Variation of Γ with e for three families of solutions of the system (37) which all pass through the value $\Gamma = 7.79$.

Table 2
Numerical values of x_0, x_1 and x_2 for the three families of solutions of (37) shown in Fig. 6

e	Γ	x_0	x_1	x_2
1.00	4.6033	4.7124	0.5880	0.5880
0.95	4.8309	4.9348	0.3804	0.7455
0.90	5.0590	5.1582	0.1705	0.9086
0.85	5.2898	5.3846	−0.0438	1.0783
0.80	5.5249	5.6157	−0.2640	1.2551
0.75	5.7660	5.8530	−0.4916	1.4400
0.70	6.0144	6.0978	−0.7279	1.6336
0.65	6.2715	6.3514	−0.9745	1.8369
0.60	6.5387	6.6153	−1.2326	2.0509
1.00	4.6033	4.7124	3.1416	3.1416
0.95	4.5853	4.6948	3.1416	3.1416
0.90	4.5662	4.6762	3.1416	3.1416
0.85	4.5459	4.6563	3.1416	3.1416
0.80	4.5242	4.6352	3.1416	3.1416
0.75	4.5010	4.6125	3.1416	3.1416
0.70	4.4760	4.5882	3.1416	3.1416
0.65	4.4492	4.5620	3.1416	3.1416
0.60	4.4201	4.5338	3.1416	3.1416
1.00	4.6033	4.7124	5.6952	5.6952
0.95	4.6273	4.7358	5.7170	5.6789
0.90	4.6522	4.7601	5.7398	5.6622
0.85	4.6783	4.7856	5.7636	5.6452
0.80	4.7056	4.8122	5.7885	5.6278
0.75	4.7344	4.8404	5.8146	5.6102
0.70	4.7650	4.8704	5.8419	5.5927
0.65	4.7978	4.9024	5.8705	5.5753
0.60	4.8332	4.9371	5.9004	5.5585

values of the roots x_0, x_1 and x_2 are given in the first table of Table 4. In reference to Fig. 8 we make the following comments. Firstly, the Γ values obtained for this family are well in accord with those values for which oscillons have been observed. Secondly, the value $\Gamma = 2.55$ occurring

Table 3
Numerical values of x_0, x_1 and x_2 for the three families of solutions of (37) shown in Fig. 7

e	Γ	x_0	x_1	x_2
1.00	7.7897	7.8540	3.1416	3.1416
0.95	7.8001	7.8643	3.1416	3.1416
0.90	7.8111	7.8752	3.1416	3.1416
0.85	7.8225	7.8866	3.1416	3.1416
0.80	7.8346	7.8986	3.1416	3.1416
0.75	7.8474	7.9112	3.1416	3.1416
0.70	7.8609	7.9246	3.1416	3.1416
0.65	7.8751	7.9387	3.1416	3.1416
0.60	7.8902	7.9357	3.1416	3.1416
1.00	7.7897	7.8540	6.7673	6.7673
0.95	7.7766	7.8410	6.7532	6.7832
0.90	7.7626	7.8271	6.7379	6.7996
0.85	7.7478	7.8124	6.7213	6.8164
0.80	7.7318	7.7966	6.7034	6.8337
0.75	7.7146	7.7795	6.6842	6.8513
0.70	7.6960	7.7610	6.6636	6.8690
0.65	7.6755	7.7408	6.6414	6.8869
0.60	7.6530	7.7184	6.6178	6.9045
1.00	7.7897	7.8540	8.6410	8.6410
0.95	7.7939	7.8582	8.6487	8.6340
0.90	7.7983	7.8626	8.6565	8.6265
0.85	7.8030	7.8672	8.6646	8.6183
0.80	7.8079	7.8720	8.6729	8.6095
0.75	7.8130	7.8771	8.6814	8.5998
0.70	7.8185	7.8825	8.6901	8.5891
0.65	7.8242	7.8882	8.6991	8.5774
0.60	7.8302	7.8941	8.7083	8.5644

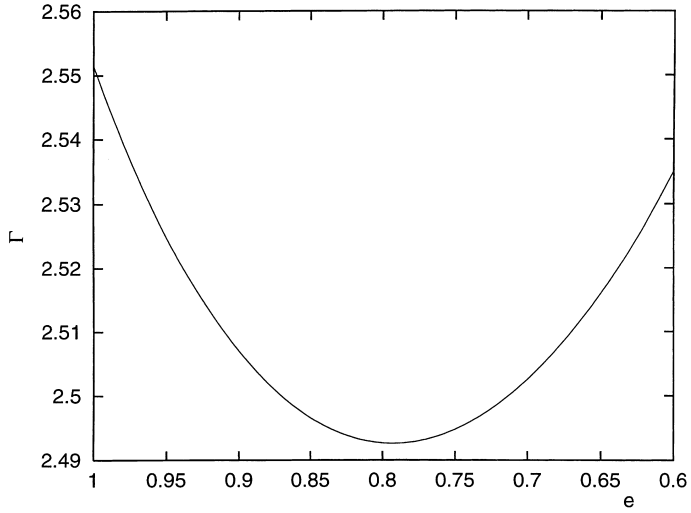

Fig. 8. Variation of Γ with e for one family of solutions of the system (37) in the range of Γ values for which oscillons have been observed to occur experimentally.

for $e = 1$ and $x_1 = x_2$ is not determined from the analysis of the previous section because it does not arise from the case $T_1 = T_2$, but rather from the alternative possibility $T_1 T_2 = 2(h_2 - h_1)/g$. They are many other similar families of solutions of (37) and two further families are shown in

Table 4
Numerical values of x_0, x_1 and x_2 for the three families of solutions of (37) shown in Figs. 8 and 9

e	Γ	x_0	x_1	x_2
1.00	2.5514	2.7500	2.5377	0.04480
0.95	2.5248	2.7255	2.5932	0.11598
0.90	2.5070	2.7092	2.6431	0.19112
0.85	2.4966	2.6997	2.6889	0.27021
0.80	2.4927	2.6961	2.7315	0.35339
0.75	2.4948	2.6981	2.7714	0.44093
0.70	2.5026	2.7052	2.8092	0.53316
0.65	2.5160	2.7175	2.8451	0.63058
0.60	2.5351	2.7350	2.8793	0.73376
1.00	4.2192	4.3383	4.2690	5.7148
0.95	4.2309	4.3496	4.2276	5.6982
0.90	4.2428	4.3612	4.1853	5.6803
0.85	4.2549	4.3729	4.1422	5.6609
0.80	4.2671	4.3848	4.0981	5.6398
0.75	4.2793	4.3967	4.0529	5.6168
0.70	4.2915	4.4086	4.0067	5.5915
0.65	4.3035	4.4202	3.9592	5.5637
0.60	4.3151	4.4315	3.9105	5.5327
1.00	4.9085	5.0108	5.8613	4.1225
0.95	4.9204	5.0224	5.8790	4.1535
0.90	4.9334	5.0351	5.8973	4.1865
0.85	4.9478	5.0492	5.9160	4.2218
0.80	4.9636	5.0647	5.9353	4.2597
0.75	4.9811	5.0819	5.9551	4.3003
0.70	5.0006	5.1010	5.9755	4.3441
0.65	5.0224	5.1223	5.9965	4.3915
0.60	5.0467	5.1461	6.0181	4.4429

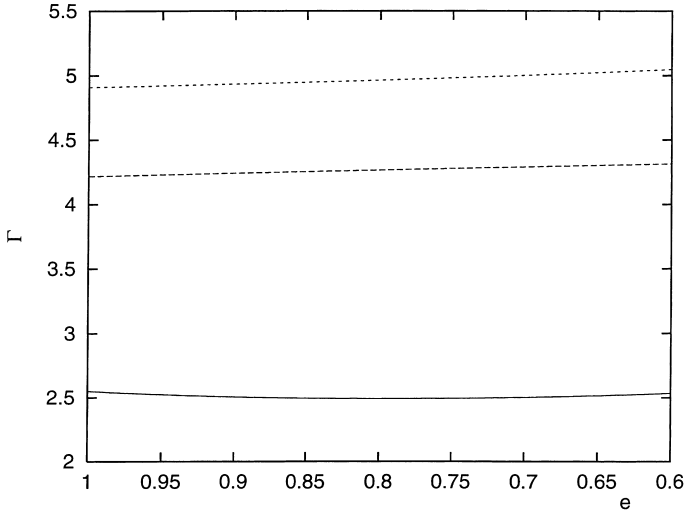

Fig. 9. Variation of Γ with e for three families of solutions of the system (37) for which $x_1 \neq x_2$ when $e = 1$.

Fig. 9 with the corresponding numerical values given in the second and third tables of Table 4. Fig. 10 shows the variation of Γ with e corresponding to $x_1 = x_2 = \pi$ for which $x_0 = \pi/2$ when $e = 1$ and the corresponding numerical data is shown in Table 5.

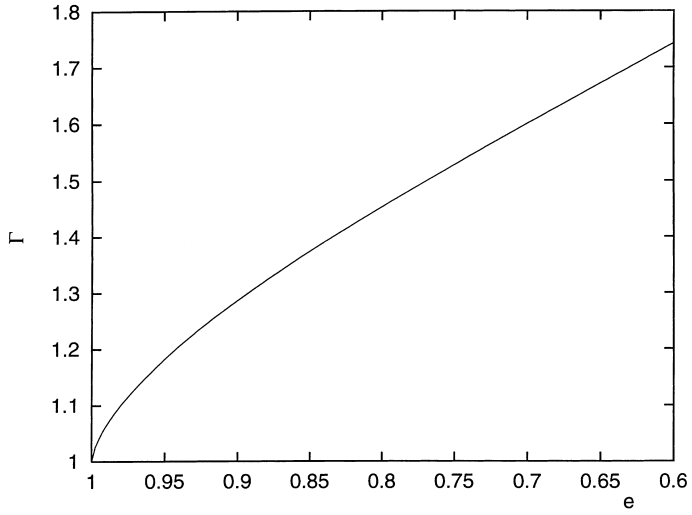

Fig. 10. Variation of Γ with e for a family of solutions of the system (37) for which $x_1 = x_2 = \pi$ and $x_0 = \pi/2$ when $e = 1$.

Table 5
Numerical values of x_0, x_1 and x_2 for the family of solutions of (37) shown in Fig. 10

e	Γ	x_0	x_1	x_2
1.00	1.0000	1.5708	3.1416	3.1416
0.95	1.1826	1.6390	3.1416	3.1416
0.90	1.2864	1.6997	3.1416	3.1416
0.85	1.3739	1.7573	3.1416	3.1416
0.80	1.4532	1.8134	3.1416	3.1416
0.75	1.5281	1.8689	3.1416	3.1416
0.70	1.6005	1.9245	3.1416	3.1416
0.65	1.6717	1.9808	3.1416	3.1416
0.60	1.7426	2.0383	3.1416	3.1416

6. Conclusion

In order to gain some insight into the problem of oscillon formation in a rapidly vibrating granular layer, we have examined the dynamics of a single particle bouncing on a horizontal plane, which itself is oscillating with amplitude A and angular frequency ω (namely $z(t) = A\sin\omega t$). Clearly, there are huge differences between the two problems, and yet the motion of an individual particle of the oscillon performs essentially the phenomena described here for an isolated bouncing ball. The oscillon is remarkable because the interactions between particles appear to be well organized so that together their individual motion is coordinated to form a continuous movement in both space and time. For $T_1 = T_2$ the mathematical analysis presented here requires that the bouncing ball be perfectly elastic and predicts an acceleration amplitude $\Gamma = A\omega^2/g$ of about 4.6 for oscillonic behavior to occur. However, for $T_1 \neq T_2$ the system of equations (37) has at least one family of solutions, which is shown in Fig. 8, for which the Γ values are precisely those observed experimentally, namely Γ in the vicinity of 2.5.

There are two approaches to our theory. Either we can attempt to properly mimic the oscillon problem and start the particle initially at rest on the plate or alternatively we can simply locate the

particle in one or other of the two stationary positions at some prescribed time t_0. In the latter case the theory predicts that perfect oscillonic behavior can occur for any amplitude A and angular frequency ω. The former interpretation is more interesting because it genuinely models the individual particles of the oscillon, assuming no interaction between particles. For the former approach we emphasize three important features of our analysis. Firstly, there are no individual restrictions on A and ω separately, but only on the combination of these quantities arising in the acceleration amplitude $\Gamma = A\omega^2/g$. Secondly, there are an infinite family of allowable Γ's and these numerical values might provide a guide for future experimentation. Thirdly, this theory does not predict perfect oscillonic behavior and we have adopted the terminology "almost" oscillonic behavior. By this we mean that for a particle initially at rest on the plate, we require the first stationary position z_0 to coincide with one of the stationary modes, namely either height h_1 or h_2. For $T_1 = T_2$ and those values of Γ which allow oscillonic behavior, the particle does not achieve this precisely, but the numerical results demonstrate in a remarkable fashion, that z_0 is almost h_1 but never h_2, assuming that $h_1 > h_2$.

We emphasize here, that clearly we have not attempted to model the oscillon as such. Rather we have attempted to gain insight into this complex physical phenomenon by examining the conditions under which an isolated particle behaves in a similar manner. We have shown that this simple analysis gives rise to specific values of Γ which might serve as a guide for future oscillon experiments.

Acknowledgements

The authors are grateful to the referees of a previous version of this paper for many helpful comments. JMH gratefully acknowledges the Australian Research Council for providing a Senior Research Fellowship. DVT and KAW are grateful to the Centre for Engineering and Industrial Mathematics and the School of Mathematics and Applied Statistics for providing Summer Vacation Scholarships. Professor Philip Broadbridge has materially aided this research and it is a pleasure to record our gratitude.

Appendix A. Asymptotic formulae for large Γ

In order to confirm the behavior indicated in Table 1, we note the following asymptotic results, which apply for large values of the parameter Γ. From Eq. (6), we may deduce

$$\omega t_0 = \Gamma + \frac{1}{2\Gamma} + \mathrm{O}\left(\frac{1}{\Gamma^3}\right), \tag{A.1}$$

and since $\omega t_0 = (2k+1)\pi/2$, it is not difficult to deduce

$$\Gamma = \pi k + \frac{\pi}{2} - \frac{1}{2\pi k} + \mathrm{O}\left(\frac{1}{k^3}\right). \tag{A.2}$$

Examination of the numerical data for the two roots of (31) (with $p = 1$) for which the quantity Δ_1 approaches zero, shows that λ is approximately $(2k-1)\pi/2$ and therefore we look for approximate roots of (31) of the form

$$\lambda \simeq (2k-1)\frac{\pi}{2} + \frac{a}{k^\alpha}, \tag{A.3}$$

Table 6
Exact and approximate numerical values of Γ and the two roots λ of (31) for which Δ_1 approaches zero (approximate values determined by the asymptotic results (A.2) and (A.4))

k	Γ		λ_1		λ_2	
	Exact	Approximate	Exact	Approximate	Exact	Approximate
5	17.2498	17.2469	14.6890	14.7696	13.4617	13.5047
10	32.9716	32.9708	30.2540	30.2923	29.3736	29.3979
15	48.6844	48.6841	45.8933	45.9182	45.1708	45.1879
20	64.3949	64.3947	61.5589	61.5773	60.9316	60.9448
25	80.1044	80.1042	77.2374	77.2519	76.6754	76.6862
30	95.8134	95.8133	92.9232	92.9352	92.4096	92.4188

where a and α are to be determined. On substituting (A.3) into (31) we may readily deduce $\alpha = 1/2$ and $a = \pm\sqrt{2}$ so that

$$\lambda_1 = \pi k - \frac{\pi}{2} + \left(\frac{2}{k}\right)^{1/2} + \mathrm{O}\left(\frac{1}{k}\right),$$
$$\lambda_2 = \pi k - \frac{\pi}{2} - \left(\frac{2}{k}\right)^{1/2} + \mathrm{O}\left(\frac{1}{k}\right). \tag{A.4}$$

The approximate and exact values of Γ, λ_1, and λ_2 are shown in Table 6 for various values of k, and of course the agreement improves with increasing k. From the asymptotic expressions (A.2) and (A.4) we may show that Δ_1 as defined by Eq. $(35)_1$, has the following asymptotic values corresponding to the two roots λ_1 and λ_2, thus

$$\Delta_{11} = -\frac{5}{4k} - \frac{\sqrt{2}}{2\pi k^{3/2}} + \frac{1}{8\pi^2 k^2} + \mathrm{O}\left(\frac{1}{k^{5/2}}\right),$$
$$\Delta_{12} = -\frac{5}{4k} + \frac{\sqrt{2}}{2\pi k^{3/2}} + \frac{1}{8\pi^2 k^2} + \mathrm{O}\left(\frac{1}{k^{5/2}}\right), \tag{A.5}$$

which confirms the behavior suggested by the numerical values given in Table 1.

References

[1] P.B. Umbanhowar, F. Melo, H.L. Swinney, Localized excitations in a vertically vibrated granular layer, Nature 382 (1996) 793–796.
[2] M. Chown, A pattern emerges, New Scientist 155 (1997) 34–37.
[3] H.M. Jaeger, S.R. Nagel, R.P. Behringer, The physics of granular materials, Physics Today (1996) 32–38.
[4] L.S. Tsimring, I.S. Aranson, Localized and cellular patterns in a vibrated granular layer, Physical Physical Review Letters 79 (1997) 213–216.
[5] N.B. Tufillaro, T. Abbott, J. Reilly, An Experimental Approach to Nonlinear Dynamics and Chaos, Addison-Wesley, New York, 1992.
[6] N.B. Tufillaro, T.M. Mells, Y.M. Choi, A.M. Albano, Period doubling boundaries of a bouncing ball, Journal de Physique 47 (1986) 1477–1482.
[7] N.B. Tufillaro, A.M. Albano, Chaotic dynamics of a bouncing ball, American Journal of Physics 54 (1986) 939–944.
[8] T.M. Mells, N.B. Tufillaro, Strange attractors of a bouncing ball, American Journal of Physics 55 (1987) 316–320.
[9] C.N. Bapat, S. Sankar, N. Popplewell, Repeated impacts on a sinusoidally vibrating table reappraised, Journal of Sound and Vibration 108 (1986) 99–115.
[10] A. Mehta, J.M. Luck, Novel temporal behavior of a nonlinear dynamical system: the completely inelastic bouncing ball, Physical Review Letters 65 (1990) 393–396.